CHARACTERIZATION OF FACTORS THAT AFFECT THE ENTRY PATHWAY OF NEGATIVELY CHARGED LIPOSOMES INTO HELA CELLS AND THEIR CELL BEHAVIOUR

With the help of: prof. dr. Anna Salvati and Catharina Reker-Smit

Author: Elise Lammers, S3891585
Examiner: prof. dr. A. Salvati
Department: Nanomedicine and Drug Targeting
Date: June 23, 2022

1. Abstract

Liposomes are compatible for drug delivery inside the human body to specific tissues due to their small size and hydrophobic and hydrophilic behaviour. In this study the uptake pathway of negative liposomes into cervical cancer cells (HeLa cells) is studied. The aim of this research is to get a better understanding of the factors that play a role in the entry pathway of negative liposomes into cells in vivo. First, sodium azide (NaAz) was used to characterize to what extent negative liposomes are taken up via active transport into HeLa cells. Subsequently, six inhibitors were used to observe via which mechanisms these liposomes enter the cells. The negative liposomes were labeled with the fluorescent dye tetramethyl indocarbocyanine perchlorate (DiI) to analyze the data with flow cytometry. It was found that depletion of ATP levels inside the cells, the internalization of negative liposomes into cells reduced with >50%. Different factors play a role in the active transport of liposomes over the plasma membrane. These include, involvement of actin and microtubules inside cells. Also, the fission of endocytic vesicles and the Na+/H+ exchanger pump in the cell membrane of HeLa cells play an important role.

Table of Contents

2. Introduction

2.1. Nanomedicines

Nanotechnology is specified as "the deliberate design, description, manufacture, and use of materials, structures, electronics, and systems in the nanoscale range (1 – 100 nm) by regulating their size and shape." Nanotechnology has the potential to be suitable for medical applications since nanoparticles are comparable in size as biological molecules and systems and can be created to perform a variety of functions. Nanomedicine attempts to diagnose and treat diseases at the molecular level by utilizing the physicochemical and physical features of nanoparticles (Kim et al., 2010).

Organic, metallic or polymeric nanoparticles, or liposomes are commonly used as nanoparticles to study drug-delivery into specific tissues inside the human body (Mirza & Siddiqui, 2014). In this study, liposomes are used for drug-delivery and are explained in further detail in the next paragraph.

2.2. Liposomes

Liposomes were the first sphere-shaped bilayer phospholipid structures to be developed in 1965. However, the first liposomal formulated approved nanomedicine was marketed 30 years later. This was Doxil, which was approved in 1995 by the US Food and Drug Administration (FDA). Doxil was used for AIDS related Kaposi's sarcoma and ovarian cancer. DaunoXome, which was developed by Nexstar Pharmaceuticals, was US FDA approved a year later (Beltrán-Gracia et al., 2019). DaunoXome was used for the transport of daunorubicin for the treatment of advanced HIV-associated Kaposi's sarcoma. As a result, more products for cancer therapy and other disorders have become marketed.

Due to the small size of liposomes, and hydrophobic and hydrophilic behaviour they are compatible for drug delivery inside the human body. Liposomes are made up of lipid bilayers that enclose aqueous units, with the polar head groups arranged in the exterior and interior aqueous pathway phases. The most liposomes for drug delivery are between 0.05 – 5.0 µm from size in diameter. Inside the aqueous core, hydrophilic agents can be enclosed. These drugs will be protected from the human body environment due to the hydrophobic core and thus early release, dilution and degradation inside the human body are prevented.

The lipid bilayer of the liposomes used for this study are made up of stiff saturated lipids, such as 1,2-dioleoyl-sn-glycero-3-phosphocholine (DOPC) and 1,2-dioleoyl-sn-glycero-3-phosphoglycerol (DOPG), and cholesterol. These lipids stabilize the bilayer and prevent the attack of plasma proteins. (Akbarzadeh et al., 2013; Allen & Cullis, 2013; Sharma, 1997). A recent study has shown that cholesterol induces the formation of specific domains inside the membrane of the liposomes that will boost delivery performance. Therefore, the drug will be delivered faster to the tissue that needs to be targeted. By changing the lipid composition, surface charge, size, and manufacturing method the delivery speed and other characteristics can be affected (Caracciolo, 2015). When these parameters are altered, liposomes can be changed in an advantageous way or either disadvantage changes can be prevented.

In this study it was chosen to choose liposomes for drug delivery since those parameters, that are mentioned before, can be adjusted easily. For example, the composition of the liposomal membrane can be changed to another ratio to charge the membrane which was done in this study. Some other advantages of liposomes for drug delivery are that liposomes have a great burden for self-assembly and are biocompatible inside the human body. They are also able to transport huge drug payloads and are very versatile (Akbarzadeh et al., 2013; Sercombe et al., 2015).

Overall, liposomes are very compatible for drug delivery inside the human body. They are used for this study since many parameters can be altered to change the behaviour of liposomes in the human body.

With this study, care must be taken that a protein corona is formed around the liposomes whenever they are placed in serum. This is a layer of proteins that normally forms around a liposome

whenever it is injected into the blood stream in the human body. Due to the corona, the biodistribution and pharmacokinetics (PK) of the liposomes are altered. The charge of the liposome itself will affect the binding of those specific proteins to the liposome. Liposomes that are charged have a higher protein adsorption rate than liposomes with a neutral charge. The ones that are cationic will absorb even more than the anionic ones (Caracciolo, 2015). Some recent studies have found that the uptake of DOPG liposomes in murine macrophages was reduced due to the protein corona (Onishchenko et al., 2021). However, it is still unclear whether liposomes enter via active transport or diffuse into the cells.

2.4. Internalization into cells

It is important to understand via which pathways negative liposomes enter the cells to optimize nanomedicine treatment further in diseased patients. When treatment is optimized, the efficacy of the drug is also increased. For this study we have used negatively charged liposomes with a ratio of 10:6.67:1 DOPC:DOPG:Cholesterol. This composition was used to see how the pathway of liposomes in HeLa cells was affected after addition of negative charge. Different methods were used to study the entry pathways of liposomes in HeLa cells. First sodium azide (NaAz) was used to study what percentage of uptake goes via active transport. NaAz depletes adenosine triphosphate (ATP) levels inside the cells. As a result, no more activities can take place in the cell that require ATP, including the active transport of liposomes into the cell (Ishikawa et al., 2006). After performing this experiment, it is known how much percent active processes play a role in the uptake of negative liposomes into the cells.

To study via which active uptake pathways the negatively charged liposomes entered the cells, six pharmacological inhibitors were used. These specific inhibitors were chosen since their dosages and kinetics were already optimized in a previous study (Francia et al., 2019). The used inhibitors and their mechanisms of action (MOA) can be found in table 1. These inhibitors were added to the cells and the uptake of the liposomes to the cells was analyzed afterwards. Nonetheless, when one pathway of internalization is inhibited, cells may modify and will upregulate different mechanisms that are normally less of interest. Thus, when no inhibition in the analysis is seen, several pathways can play a role in this process. Therefore, it may be hard to interpret the results and draw conclusions.

Table 1: Overview of inhibitor, their MOA and affected pathways (Francia et al., 2019).

Inhibitor	MOA	Pathways
Chlorpromazine hydrochloride	Inhibits adaptor protein 2 (AP-2).	Clathrin-mediated endocytosis (CME)
Cytochalasin D	Binds F-actin and blocks polymerization	CME, macropinocytosis, clathrin-independent endocytosis (CIE)
Nocodazole	Binds to tubulin and prevents polymerization of microtubules.	CME, macropinocytosis and other pathways.
5-(N-Ethyl-N-isopropyl)amiloride	Inhibition Na+/K+ pump on the cell membrane	Macropinocytosis
Dynasore	Inhibition dynamin	Several pathways
Methyl-ß-cyclodextrin	Cholesterol depletion	Several pathways

Chlorpromazine (CP) is known to inhibit the clathrin-mediated endocytosis of the liposomes into the cells. This pathway is inhibited through the inhibition of adaptor protein 2 (AP-2) (Francia et al., 2019). To understand why the inhibition of AP-2 leads to the inhibition of this specific pathway, the mechanism is explained in more detail. The clathrin-mediated endocytosis (CME) involves four steps: the initiation step; propagation of the coated liposome; budding of the vesicle; uncoating of the vesicle when it is inside the cell. Chlorpromazine is acting on the propagation step on this process. This step involves the coating of liposomes by clathrin. Clathrin does not directly bind to the membrane but it links the membrane to the liposome with AP complexes. A member of this family is the AP-2

complex which mediates endocytosis (Godlee & Kaksonen, 2013; Royle, 2006). When chlorpromazine is used as an inhibitor, the coating of liposomes with clathrin is prevented. Therefore, the endocytosis of liposomes into cells is prevented.

The mycotoxin cytochalasin D (CytD) binds to the ends of F-actin, resulting in the formation of aggregates which blocks the polymerization of actin. Normally, actin filaments are below the plasma membrane. Here, the filaments form a structure which gives mechanical support to the cells and these structures also determine the shape of the cell. Also, they allow the movement of cells and the mitosis of cells (Cooper GM., 2000b). Eventually, the blockage of the polymerization step leads to an immediate disruption of the cytoskeleton (Francia et al., 2019; Schliwa, 1982). Therefore, by adding this inhibitor to the HeLa cells it is studied whether maintenance of the cytoskeleton contributes to the uptake of liposomes into the HeLa cells. The addition of cytochalasin D to cells also inhibits another process. When actin is polymerized at the cell membrane and 'actin ruffles' are formed, macropinocytosis is initiated (see figure 1). Due to the inhibition of the polymerization reaction, macropinocytosis is inhibited (Canton, 2018; Francia et al., 2019; Lin et al., 2020).

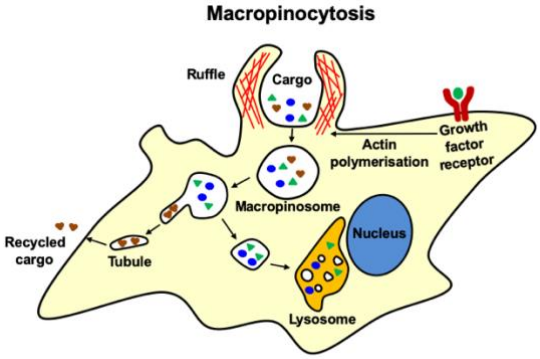

Figure 1: Pathway macropinocytosis (Singh et al., 2017).

Nocodazole (ND) is a microtubule-depolymerizing agent by binding to tubulin (Blajeski et al., 2002; Francia et al., 2019). Nocodazole binds to α and β monomers and this will prevent the polymerization of tubulin into microtubules. This leads to a G1 and G2 cell cycle arrest and therefore inhibition of the cell division and growth (Binarová & Tuszynski, 2019; Cooper GM., 2000a). Several processes are inhibited due to this. Microtubules also interact with actin inside the cell. As mentioned earlier, actin determines the cell shape. Because microtubules constantly grow or shorten, they are more dynamic than actin. Interaction between actin and microtubules is necessary to support some important processes inside the cell. These processes include the formation and maintenance of the cell shape; cell division and migration; interactions and transport intracellularly (Dugina et al., 2016). It is hypothesized that when this inhibitor is added to HeLa cells, the cytoskeleton will be affected. Micropinocytosis is also inhibited when using this inhibitor. By adding this inhibitor to the cells, it is checked whether the arrest of the cell cycle influences the uptake of liposomes into the cells.

5-(N-Ethyl-N-isopropyl)amiloride (EIPA) is inhibiting the Na+/K+ exchanger pump that is located inside the cell membrane. This leads to an altered pH in and around the cell where macropinosomes are being formed. Higher concentrations of H+ are now inside the cell which decreases the pH of the cell. Therefore, it is hypothesized that more cell dead may be observed. EIPA also has another inhibiting effect, namely the inhibition of Cdc42 and Rac1 signaling. These signals are fundamental for macropinocytosis. Overall, this leads to the inhibition of macropinocytosis (Francia et al., 2019).

Dynasore (Dyn) is used to block the key protein dynamin. This is an essential protein for the fission of endocytic vesicles from the plasma membrane. The protein wraps itself around the 'neck' of the vesicle and converts the GTP that was bound to GDP. The constriction mechanism of the GTPase domain then induces membrane fission (Singh et al., 2017). Several pathways are therefore inhibited by Dynasore (Francia et al., 2019).

Lastly, Methyl-ß-cyclodextrin (MBCD) depletes the cells cholesterol levels. As mentioned earlier, the plasma membrane consists for a big part out of cholesterol. When these levels are depleted, the cell loses its stability and permeability (Francia et al., 2019). When this inhibitor is added, it can be studied whether cholesterol needs to be in the plasma membrane for the active uptake of liposomes into the cells.

Overall, the aim of this research is to get a better understanding of the factors that play a role in the entry pathway of negative liposomes into cells in vivo. How much of the uptake goes via active transport is first studied using NaAz. Subsequently, the different factors that play a role in the entry pathways are examined using six pharmacological active inhibitors. As mentioned earlier, all conditions are already optimized in a previous study.

3. Methods

3.1. Liposome preparation

The lipids that were used were bought from Avanti Polar Lipids. The dye that was used to stain the lipids is 1 mg/mL 3,3'-dioctadecylindocarbocyanine-labeled (Dil) from ThermoFisher Scientific. For the negatively charged liposomes a composition of 10:6.67:1 of 1,2-dioleoyl-sn-glycero-3-phosphocholine (DOPC, Avanti Polar Lipids):1,2-dioleoyl-sn-glycero-3-phosphoglycerol (DOPG, Avanti Polar Lipids):Cholesterol (Avanti Polar Lipids) was used. First 20 mg of the 10:6.67:1 DOPC:DOPG:Chol stock was dispensed a tube and dissolved in chloroform until the concentration reached 10 mg/mL. This solution was stored at -20 degrees Celsius. After mixing the solution, it was dried under nitrogen gas. The liposome stock and lipid dye were stored in a glass vial with aluminum foil around it overnight under vacuum at room temperature. After 24h, 1 mL of phosphate-buffered saline (PBS) was added to the dried lipid. The tube with PBS and the dried lipid was then placed in a sonicator to dissolve the pellet. After the pellet was dissolved, the solution was freezed under liquid nitrogen and thawed in a water bath at 37 degrees Celsius for at least 8 times to fuse the membranes together. After freeze-thawing, the extruder with a filter of 100 nm was used for at least 21 times to extract the liposomes. After extruding the stock concentration of the first batch liposomes was determined to be 9.0 mg/mL. The second batch that was made had a stock concentration of 11.56 mg/mL. Those concentrations were calculated using a calibration line for different concentrations of liposomes ranging from 1 – 100 µg/ml.

3.2. Cell culture HeLa cells

Human cervical cancer cells (HeLa cells, ATCC CCL-2TM) were used in this experiment. For the cell splitting procedure first the complete minimum essential medium (cMEM), PBS and 0.5% trypsin-EDTA (TEP) were obtained. cMEM was made by adding 10% fetal bovine serum (FBS, Gibco) to MEM (Gibco). The cMEM which is in the T75 flask with the inoculated cell culture first needs to be removed. Then, the cells will be washed two times with PBS and afterwards the cells will be released from the bottom of the flask using 3 mL TEP and by incubation for 5 minutes (min) at 37 degrees. After incubation, the cells will be rinsed with 2 times with 5 mL cMEM and put into a 50 mL tube. This tube will be centrifuged at 300g for 5 min. When a cell pellet is observed after centrifugation the supernatant can be extracted and 10mL cMEM can be added into the tube. Afterwards, the cell count is performed. The HeLa cells are grown into a T25 flask at 37 degrees Celsius with a CO2 level of 5%. The HeLa cell line was used for a maximum of 20 passages after being defrosted.

3.3. Chemical inhibitor exposure and uptake studies

The HeLa cells were pipetted into the wells with a density of 50.000 cells/well in the 24-wells plate (Greiner Bio-One), 24 hours before the experiment. Starting the experiments, the cells were pre-incubated with the inhibitors for 20 minutes (CP, CytD, ND and EIPA) or for 1h (Dyn and MBCD). As follows, the optimized dosages that were used for pre-incubation: CP 10 µg/mL (Sigma-Aldrich); CytD 2.5 µg/ml (ThermoFisher Scientific); ND 5 µM (Biovision); EIPA 100 µM (Sigma-Aldrich); Dyn 25 µg/ml (Biovision) and 2.5 MBCD mg/mL (Sigma-Aldrich). CP, CytD, ND and EIPA were pre-incubated in cMEM and Dyn and MBCD in serum free MEM (SF-MEM). After pre-incubation with the drugs, the liposomes were added to the cells with and without the inhibitor drugs. The efficacy of the inhibitors was assessed using flow cytometry. This is explained in more detail in the next section. 1 µg/mL C5-Lactosylceramide/BSA complex (LacCer, Thermo Fisher Scientific) was used as a positive control for MBCD in serum free MEM. For EIPA, the positive control was 250 µg/mL Dextran (ThermoFisher Scientific) in cMEM.

3.4. Analysis with flow cytometry

After exposing the HeLa cells to negatively charged liposomes, the cells were harvested for analysis. To analyze the cells first the cMEM, PBS and TEP need to be at room temperature. To minimize the presence of fluorescent particles or liposomes, the cells were washed by 1 mL cMEM and two times 500 µL PBS. To detach the cells from the bottom of the 24-wells plate, 250 µL TEP was added to the wells and the plate was set on a shaker for 5 min at 37 degrees Celsius. Afterwards, 500 µL cMEM was added to each well and the solution with cells was collected in 2 mL Eppendorf tubes. These were subsequently centrifuged for 5 min at 300g. After a cell pellet was observed the Eppendorf tubes were emptied and 100 µL PBS was added. For fluorescent labeling of the liposomes 1,1'-dioctadecyl-3,3,3',3'-tetramethylindocarbocyanine perchlorate (DiI) was used. This compound has an excitation wavelength of 550 – 552 nm and an emission wavelength of 568 – 570 nm. Therefore, the analysis on the CytoFLEX S Flow Cytometer was done in channel 585/42 BP. To eliminate cell detritus and doublets, gates were placed in the side and forward scattering plots. A minimum of 20.000 cells was required for analysis. The data that was obtained from the CytoFLEX S was analyzed using Excel and the FlowJo software.

4. Results and discussion

4.1. Liposome composition

The lipids that were used for these experiments had a composition of 10:6.67:1 DOPC:DOPG:Chol. In figure 2 the chemical structures of DOPC, DOPG and cholesterol are compared. It can be seen that DOPC is a zwitterionic (neutral) lipid due to the big phosphatidylcholine head group and the two unsaturated hydrocarbon chains. DOPG is a negatively charged lipid. The two unsaturated hydrocarbon chains resemble the ones of DOPC. However, the head group is composed of a neutral glycerol group and a phosphate group.

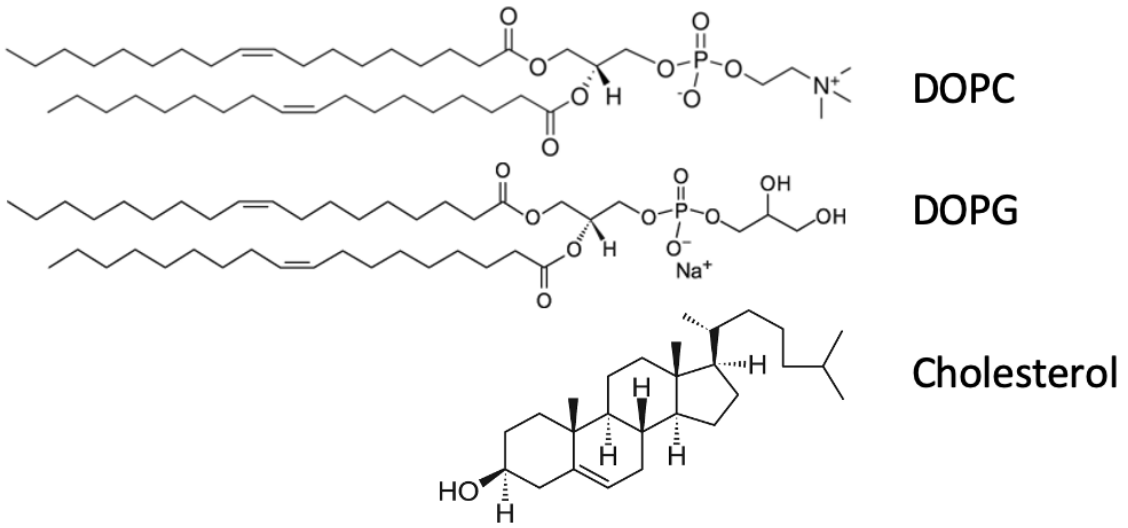

Figure 2: Chemical structures of the lipids **(SigmaAldrich, 2022; Avanti, 2022).**

To label the negative liposomes with fluorescent dye, we have used DiI. This compound has an excitation wavelength of 550 nm. The emission peak of this compound is at a wavelength of 564 nm. Therefore, the channel that was used to measure the liposomes on the flow cytometer was 585/42 BP.

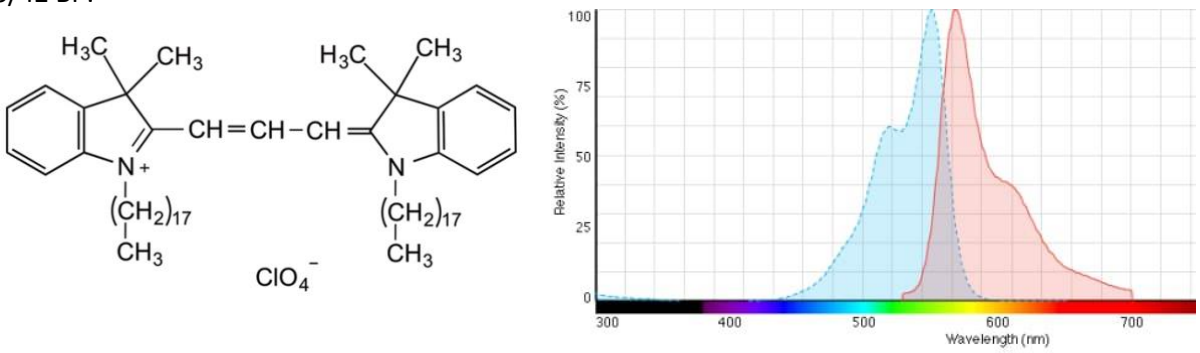

Figure 3: Chemical structure and spectrum of DiI (Cheng et al., 2014).

4.2. Size and zeta potential

The size and zeta potential of the liposomes were measured with dynamic light scattering (DLS). This method was used to determine the size distribution of nanoparticles in a solution (Stetefeld et al., 2016). It is specifically important to know what the size and charge of liposomes are in serum, since this mimics the human body environment. The size of the mean was determined to be 141.7 nm (figure 4A). The zeta potential of the liposomes in cMEM is -8.0 mV (figure 4B).

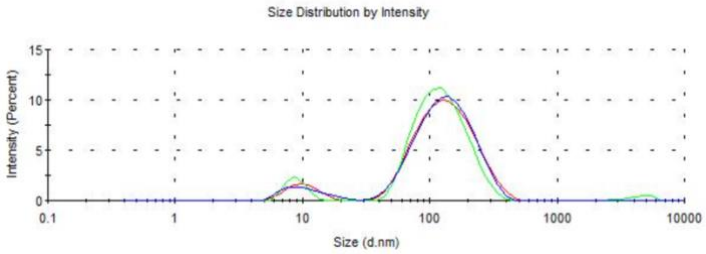

	Size (d.nm)	*Zeta (-mV)*
DOPG-DOPC-Chol in cMEM 1	147.6	-7.5
DOPG-DOPC-Chol in cMEM 2	132.4	-7.64
DOPG-DOPC-Chol in cMEM 3	145.2	-8.77

A **B**

Figure 4: DLS measurement of negative liposomes in cMEM. *A) Percent intensity plotted against the size in d.nm. of negative liposomes in cMEM. B) Raw data of size and zeta potential measured by DLS.*

4.3. Flow cytometry

As described in the previous section, flow cytometry was used to analyze the data. Flow cytometry is a reliable high throughput approach for assessing the internalization of fluorescently labeled nanoparticles in thousands of single cells in a short amount of time. The fluorescent dye that is labeled to the liposomes, scatters light in two directions: forward scatter (FSC), which reflects the cell's relative size; and at 90 degrees the side scatter (SSC), which indicates the cell's internal granularity or complexity. Fluorescence has no effect on light scatter.

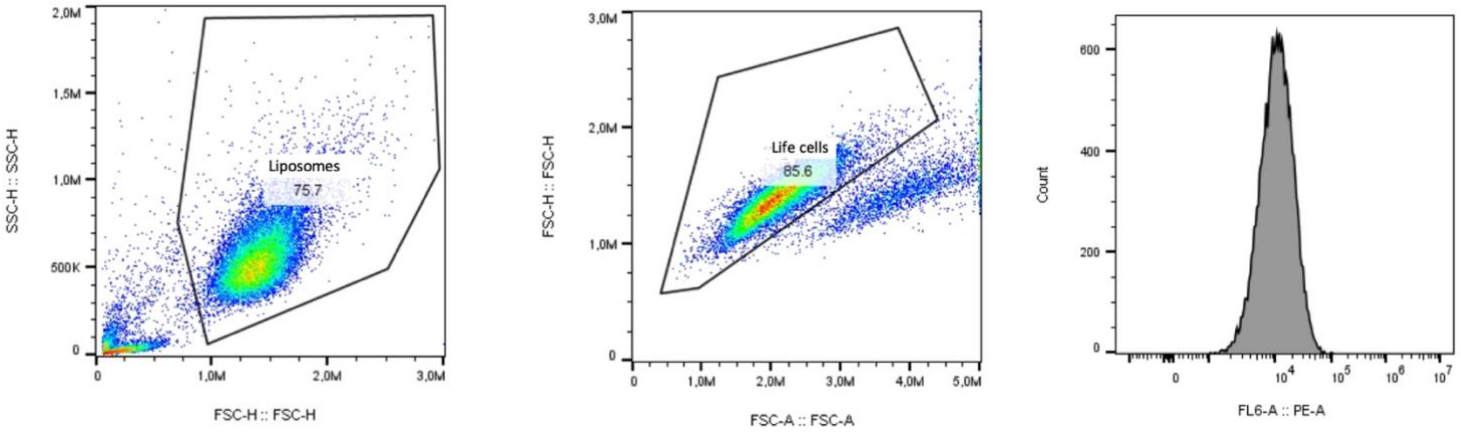

A **B** **C**

Figure 5: Flow cytometry analysis. *A) Light scattering presented in SSC-H as a function of FSC-H. B) Light scatter presented in FSH-H as a function of FSH-A. C) Cell fluorescence distribution.*

In figure 5A, side scattering height (SSC-H) is plotted as a function of forward scatter height (FSC-H) to exclude debris and dead cells. In figure 5B, forward scatter height (FSC-H) is plotted as a function of forward scatter area (FSC-A) to exclude doublets. Now only the single cells are included. The cell fluorescence distribution is shown in the histogram in figure 5C. From this histogram, the median value is taken each time to make uptake kinetic diagrams. The median represents the middle value of the peak and is indicated on the x-axis.

4.4. Uptake kinetics liposomes

For every experiment a concentration of 50 µg/mL negative liposomes were added to the HeLa cells. First, the kinetics of the negative liposomes were studied to check whether the liposomes were really taken up by the HeLa cells. To confirm that the liposomes were really taken up, this experiment was done twice, this is shown in figure 6.

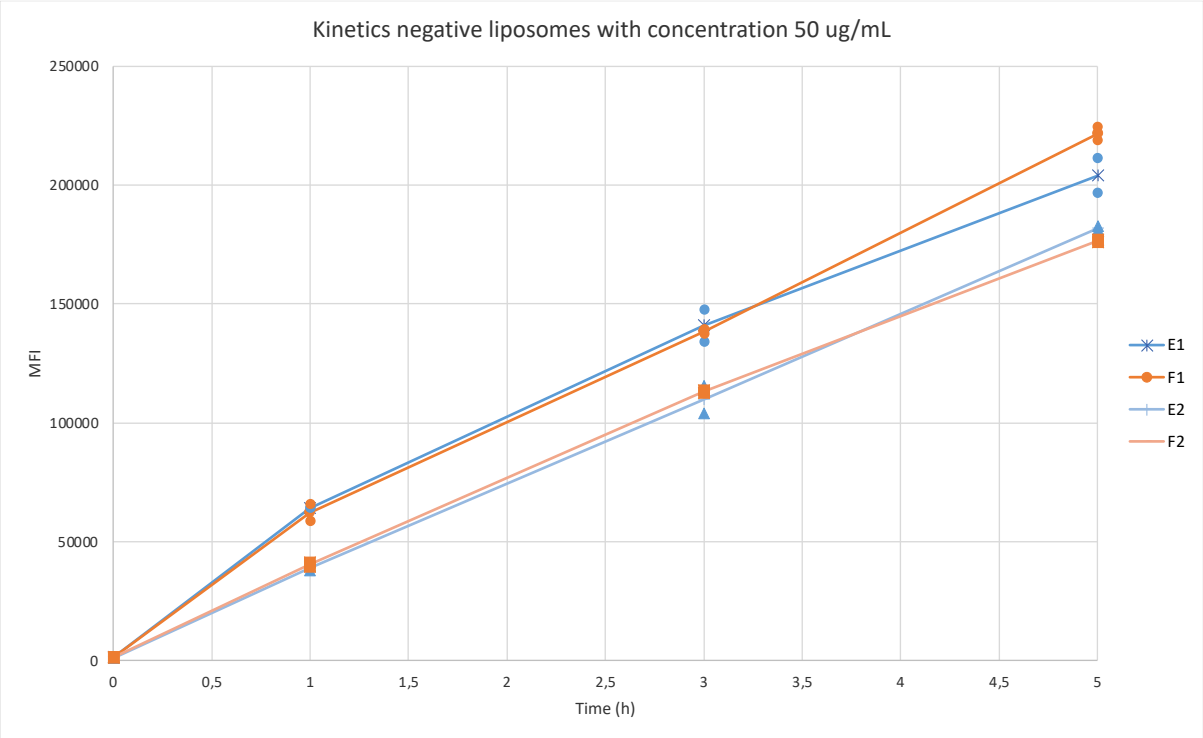

Figure 6: Cell fluorescence intensity plot as a function of time. *HeLa cells in cMEM were exposed to 50 µg/mL negatively charged liposomes in cMEM for increasing time points. The cell fluorescence was measured using flow cytometry. The results are the average of two duplicates of each person. The blue and orange lines present the replicates of Elise and Floris. The dots on each time point represent the duplicates from each person.*

The dark orange and blue lines represent the first experiment that was done and the light orange and blue represent the second experiment that was done. As can be seen, both lines show a similar uptake kinetics but the second experiment that was done showed a lower median fluorescent intensity (MFI) than the first one over time. In the first experiment, HeLa cells with a passage number of P11 + 16 were used. In the second experiment the next passage was used, namely P11 + 17. This can be an explanation for the difference between both MFI values, since for both experiments exactly the same circumstances were used. As mentioned in the method section, HeLa cells are only used until a passage number of 20 in these experiments. Therefore, it can be that the cells were exhausted since this was already the 17th passage number. This can be an explanation for the fact that liposomes were taken up less quickly by those HeLa cells instead of previous passages, however it is expected that cells with a passage number of 17 are still as active as "new" cells. Another explanation can be that both experiments were taken on another day with a different 24-wells plate with a different number of cells in them. However, it can be seen in figure 6, the duplicates (E1/F1 and E2/F2) of the two experiments do not differ much from each other and those results are reliable to use for upcoming experiments.

4.5. Uptake kinetics of liposomes with sodium azide

After it was confirmed that the negative liposomes were taken up by the HeLa cells, it was determined to what extent liposomes were transported into HeLa cells via active pathways. This was done with sodium azide (NaAz). The experiment was done twice. NaAz binds to cytochrome C oxidase which is responsible for the generation of ATP. Due to this, ATP levels inside the cells are depleted and they cannot take up liposomes via active transport anymore (Ishikawa et al., 2006). The MFI that is measured with the flow cytometer after adding NaAz to the cells, are the liposomes taken up by the cells via pathways in which ATP is not involved. This MFI may indicate lipid dye leakage, causing DiI entering the plasma membrane of the cells without liposomes. Or it could indicate that the liposomes

are stuck on the cell wall and are not washed away during the harvesting procedure. Another fact may be that the liposomes entered the cell via fusion with the plasma membrane.

In the first experiment, the cells were pre-incubated with 5 mg/mL NaAz for 20 minutes. Afterwards, liposomes with 5 mg/mL NaAz were added to the cells that were pre-incubated with NaAz. After the analysis it was observed that the ATP levels inside the cells were not depleted to such an extent as expected (see figure 7). In figure 7B the cell fluorescence after incubating the cells for 20 min with NaAz is given. After exposure of 1 hour, the cell fluorescent still remained 50%. With increasing time points, the cell fluorescence was also increasing. From literature it was suggested that a big part of liposome uptake goes via active transport into the cells. However, this was not in line with these results. This may suggest that cellular ATP levels are not depleted to a great extent after 20 minutes of pre-incubation. It could be that other pathways which do not use ATP are upregulated. To check whether this was true, the experiment was done for a second time with the same conditions, but this time with a pre-incubation for 1.5 h. The results of these experiments are shown in figure 8.

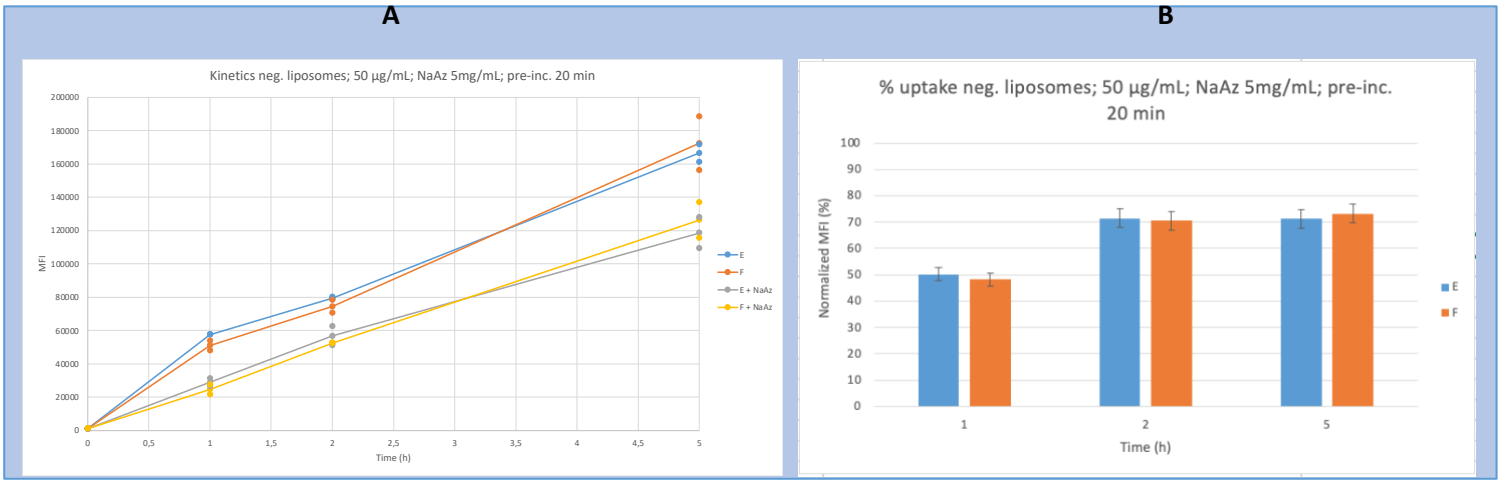

Figure 7: Sodium azide to block ATP-dependent processes inside HeLa cells. *HeLa cells were pre-incubated for 20 minutes with 5 mg/mL NaAz in cMEM and afterwards exposed to 50 µg/mL negatively charged liposomes with 5 mg/mL NaAz for increasing time points. The cell fluorescence was measured using flow cytometry. The results are the average of two duplicates of each person. The blue and orange lines represent replicates of the cell fluorescent intensity of negative liposomes in HeLa cells. The yellow and grey lines represent the cell fluorescent intensity of HeLa cells exposed to NaAz. The dots on each time point represent the duplicates from each person. A) Cell fluorescence intensity plot as a function of time. B) Data of (A) normalized for the uptake of liposomes in control cells without NaAz. The blue and orange bars are replicates of each other. The error bars present the standard error of duplicate results.*

The grey and yellow line in figure 3A and 4A indicate the uptake of negative liposomes in HeLa cells when they were pre-incubated with 5 mg/mL NaAz. The blue and orange lines represent the uptake kinetics of the liposomes into HeLa cells. The different pre-incubation times show a big difference in cell fluorescence after addition of NaAz. When the cells were pre-incubated for 20 minutes and afterwards exposed to NaAz plus liposomes for 1 h, the cell fluorescence was about 50% lower compared to the cell fluorescence of liposomes without NaAz. However, when the pre-incubation was extended to 1.5 h, the cell fluorescence reduced to 20% after 1h of exposure. Over time, the cell fluorescence decreased when the cells were pre-incubated for 1.5 h with NaAz. This was not the case for 20 min pre-incubation. This could indicate that after 1.5 h of pre-incubation the ATP levels inside the cells are depleted to a higher extent than after 20 min of pre-incubation. Another explanation is that after 1.5 h of pre-incubation a higher percentage of cells was dead which has nothing to do with the depletion of ATP levels.

Nonetheless, for the experiment with 20 min pre-incubation time, cells with a passage number of P11 + 18 were used. In the second experiment with a longer pre-incubation time, a new set of cells was used with a passage number of P11 + 5. It can be that the 'older' cells were less affected by the NaAz after 20 min since they were already exhausted. However, this is unlikely since we already exclude cells with a passage number higher than 20 and expect cells with a lower passage number than 20 to be viable. To check whether the cells were already dead after 20 min and after 1.5 h, analysis of the forward and sideward scatter of the negative liposomes was done. Those results are shown in figure 9.

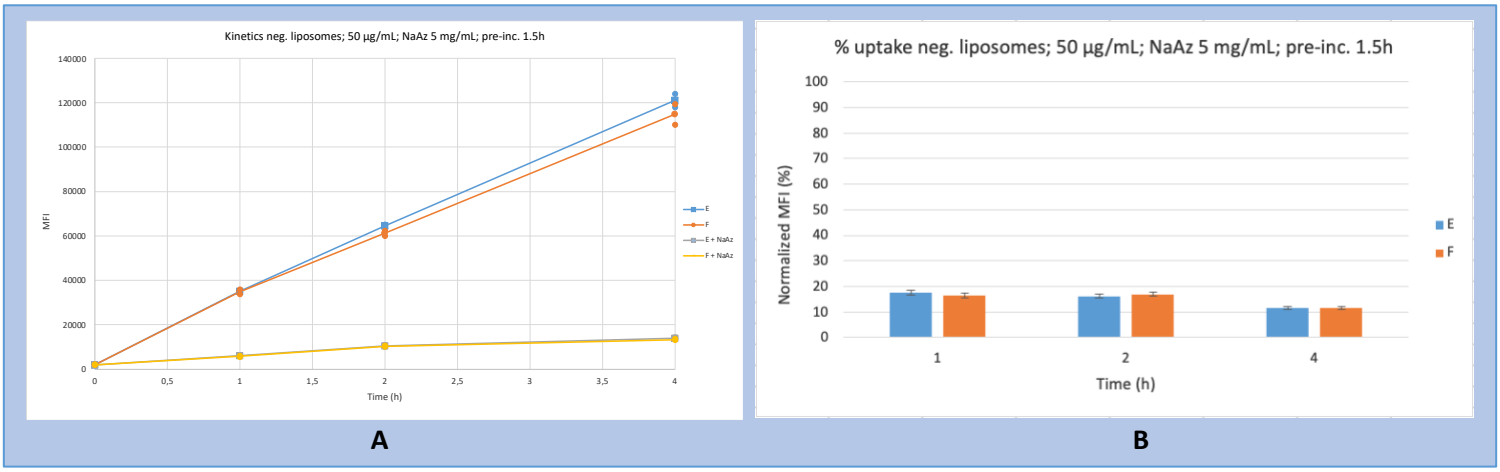

Figure 8: Sodium azide to block ATP-dependent processes inside HeLa cells. *HeLa cells were pre-incubated for 1.5 h with 5 mg/mL NaAz in cMEM and afterwards exposed to 50 µg/mL negatively charged liposomes with 5 mg/mL NaAz for increasing time points. The cell fluorescence was measured using flow cytometry. The results are the average of two duplicates of each person. The blue and orange lines represent replicates of the cell fluorescent intensity of negative liposomes in HeLa cells. The yellow and grey lines represent the cell fluorescent intensity of HeLa cells exposed to NaAz. The dots on each time point represent the duplicates from each person. A) Cell fluorescence intensity plot as a function of time. B) Data of (A) normalized for the uptake of liposomes in control cells without NaAz. The blue and orange bars are replicates of each other. The error bars present the standard error of duplicate results.*

After 5 hours of exposing the cells to liposomes with NaAz, the cell count in the first experiment with NaAz was still 20.000, which is wanted to get a reliable outcome. This indicates that still many cells are alive. In the second experiment the cell count was only around 6.500 (figure 9C). When comparing figure 9A and 9B to each other, it can be seen that figure 9B shows a higher intensity of dead cells and debris. Therefore, it can be concluded that the drop in cell fluorescence in the second experiment is related to the fact that the cells were dead after 1.5 h of pre-incubation.

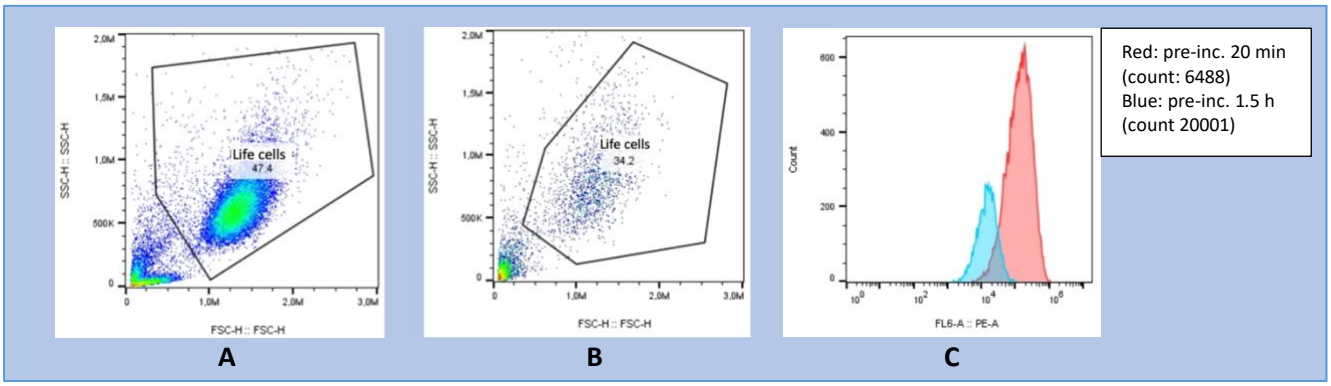

Figure 9: Flow cytometry analysis. *HeLa cells were pre-incubated with 5 mg/mL NaAz in cMEM and afterwards exposed to 50 µg/mL negatively charged liposomes with 5 mg/mL NaAz for increasing time points. The cell fluorescence was measured using flow cytometry. Scattering of cells with fluorescently labeled liposomes presented in SSC-H against FSC-H, when A) pre-incubated for 20 minutes with 5mg/mL NaAz and B) pre-incubated for 1.5h with 5 mg/mL NaAz. C) Difference in cell fluorescence distribution for different pre-incubation times with NaAz.*

To draw conclusions on what percentage of cells were actually taken up via active transport into the cells, another experiment should be done. This time another time point should be taken between 20 min and 1.5 h of pre-incubation. Then it can be seen whether the reduced uptake is really because of depleted ATP levels or due to dead cells. However, from the first experiment it was already seen that around 50% of the uptake of liposomes into cells depends on active transport. In this experiment, a large part of the cells was still alive. Therefore, it can be concluded that >50% of the uptake of negative particles into HeLa cells depends on active transport.

To study via which active pathways the negative liposomes enter the HeLa cells, six inhibitors were used. Their mechanism(s) of action and their pathway entry are summed up in table 1. The dosages that are used for all inhibitors were already optimized in a previous study which was mentioned in the introduction. The dosages and pre-incubation times that were used in the experiments are stated in the method section *"3.3. Chemical inhibitor exposure and uptake studies"*.

4.6. Uptake kinetics of liposomes with chlorpromazine

The first inhibitor that was used was chlorpromazine. The cells were pre-incubated for 20 min and afterwards exposed to liposomes with 10 µg/mL chlorpromazine. Also, some wells were only filled with liposomes to compare the uptake of negative liposomes into HeLa cells with and without the inhibitor. The results of those experiments are summed up in figure 10.

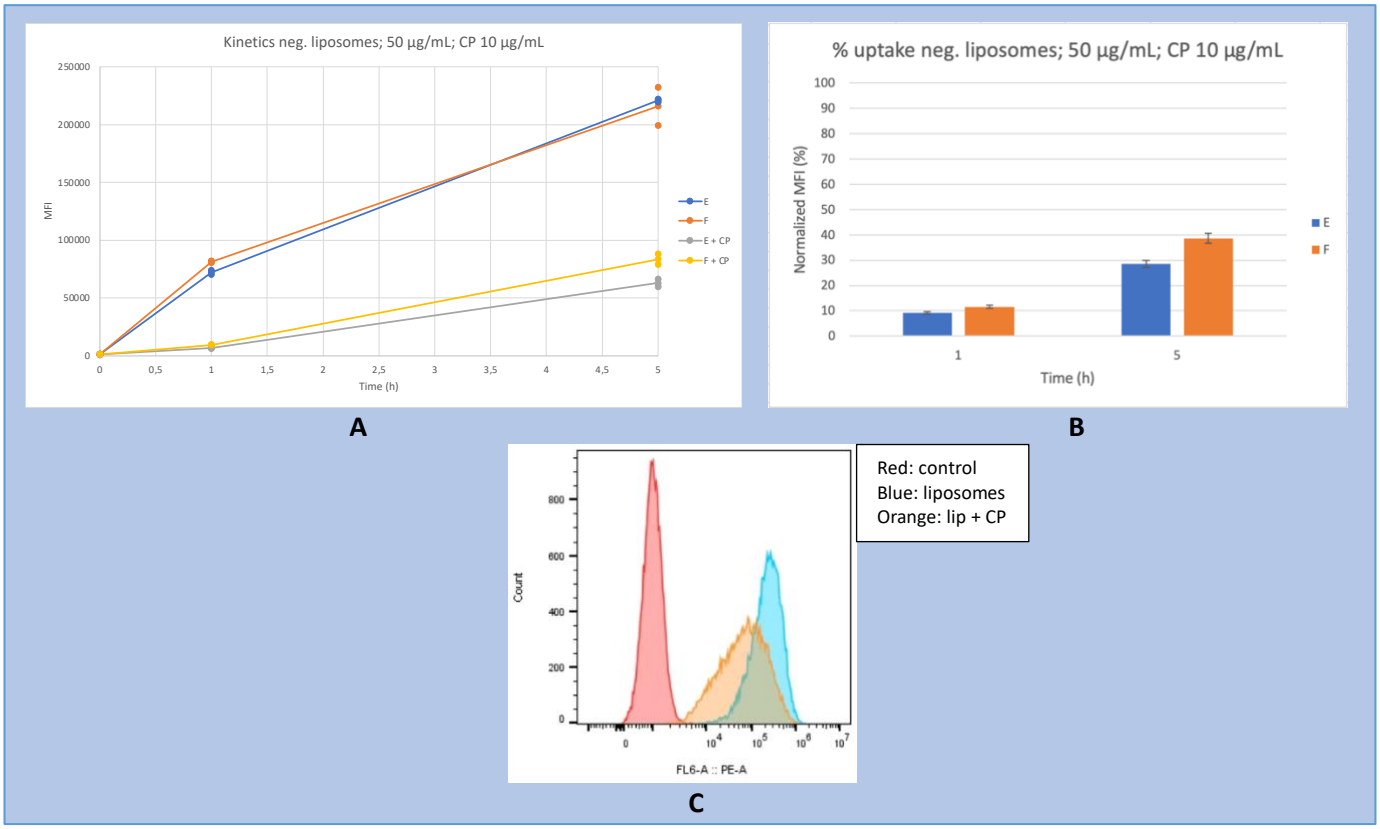

Figure 10: Chlorpromazine to block CME. *HeLa cells were pre-incubated for 20 minutes with 10 µg/mL chlorpromazine in cMEM and afterwards exposed to 50 µg/mL negatively charged liposomes with 10 µg/mL chlorpromazine for increasing time points. The cell fluorescence was measured using flow cytometry. The results are the average of two duplicates of each person. The blue and orange lines represent replicates of the cell fluorescent intensity of negative liposomes in HeLa cells. The yellow and grey lines represent the cell fluorescent intensity of HeLa cells exposed to chlorpromazine. The dots on each time point represent the duplicates from each person. A) Cell fluorescence intensity plot as a function of time. B) Data of (A) normalized for the uptake of liposomes in control cells without chlorpromazine. The blue and orange bars are replicates of each other. The error bars present the standard error of duplicate results. C) Difference in cell fluorescence distribution with (orange) and without (blue) treatment of chlorpromazine.*

As can be seen from figure 10A, the cell fluorescence was inhibited after addition of chlorpromazine. The reproducibility between me and Floris in this experiment is good since the lines are in close proximity for each time point. Also, the duplicates of each of us are very close together (dots in figure 10A). Therefore, those results are reliable to use to draw conclusions out of it. No difference in cytoskeleton was observed when the cells were treated with chlorpromazine, unfortunately no pictures were taken of this.

After 1 hour of exposure to chlorpromazine, the cell fluorescence decreased with 90% (figure 10B). However, the cell fluorescence increased over time. After 5 hours, the cell fluorescence was more than 2 times higher, around 30 – 40%. However, the inhibition is still very strong at this point since the cell fluorescence decreased with around 70% after addition of chlorpromazine. The small increase of 20 – 30% in cell fluorescence between those time points can have several reasons. Since chlorpromazine is a cationic amphiphilic drug, it may be that the drop in inhibition after 1 hour is due to the strong interaction between the two charges of the drug and the negative liposome. The increase in cell fluorescence afterwards can be explained by the fact that the charge of the liposomes may become somewhat more positive due to the interaction with the proteins in serum. Another explanation can be that HeLa cells adapt quickly to chlorpromazine and upregulate alternative pathways to let the liposomes enter the cells. Also, chlorpromazine is a low potency drug which means that more drug is needed to produce an effect. After 5 hours the effect can therefore be lost since no addition of drug to the cells was done at this time point. However, transferrin was used in a previous paper as a control for CME. This paper showed that chlorpromazine inhibited the transferrin uptake at all time points, which suggests that CME is inhibited (Francia et al., 2019). Therefore, this explanation is unlikely. Another suspicion is that CME is a pathway that is upregulated in early stages of liposome uptake. Then, after 5 h other pathways are upregulated which make the inhibitory effect of chlorpromazine on CME not useful anymore. All these factors can explain the small increase in cell fluorescence over time. In order to clarify on these possible interpretations, further research needs to be done. Multiple time points between 0 and 5 hours should be taken. When of example 10 time points are taken between these time points, the effect of CME on the early stages of liposome uptake may be seen. Also, other time points after 5 hours need to be measured to check whether the median fluorescent intensity also increases here. This may suggest the upregulation of other pathways. On the other hand, the treatment was already optimized and it may be that exposing the cells to 10 µg/mL chlorpromazine for over 5 h may be toxic to the cells. The cell viability was measured in another study and determined to be 50% for this concentration of chlorpromazine (Francia et al., 2019). It is possible that after 5 hours the cell viability will drop even further, making the results less reliable. In further studies it is useful to add transferrin and low-density lipoproteins (LDL) as a positive control for CME. These compounds show no toxicity to the cells and the cell fluorescence can be measured at later time points.

Overall, it can be concluded that chlorpromazine inhibits the internalization of negatively charged liposomes into cells by inhibiting AP2 to a great extent. This suggests that CME is involved in a great part of liposome internalization into HeLa cells.

4.7. Uptake kinetics of liposomes with cytochalasin D

The second inhibitor that was studied was cytochalasin D. This inhibitor was added in a concentration of 2.5 µg/mL to the HeLa cells. Also, in this experiment the cells were pre-incubated for 20 min with the inhibitor.

In figure 11A the uptake kinetics of liposomes into the cells are indicated. For this experiment the reproducibility between both of us is very good, for liposomes with cytochalasin D the lines even overlap which means that there is only a small difference in results. Also, the duplicates of each of us do not differ much from each other because no large spread can be observed between the points. The yellow and grey line indicate the uptake kinetics of liposomes treated with cytochalasin D, in which a great inhibitory effect is observed compared to the uptake kinetics of liposomes alone.

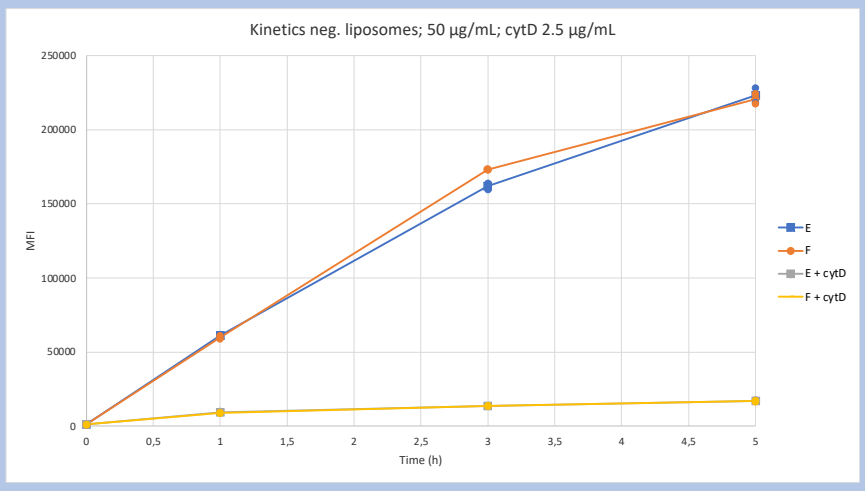

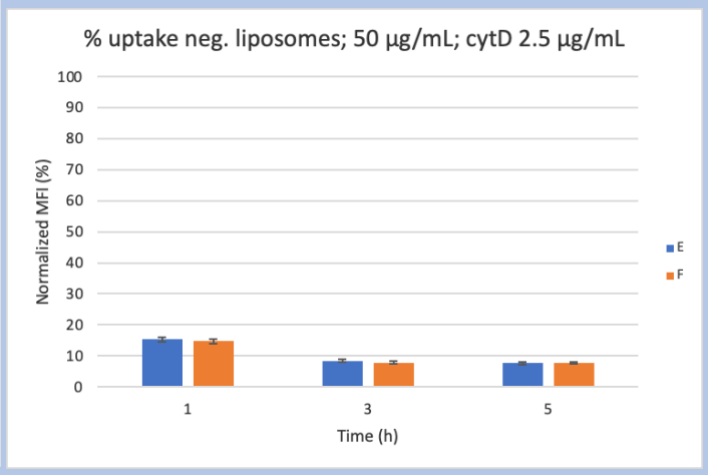

A **B**

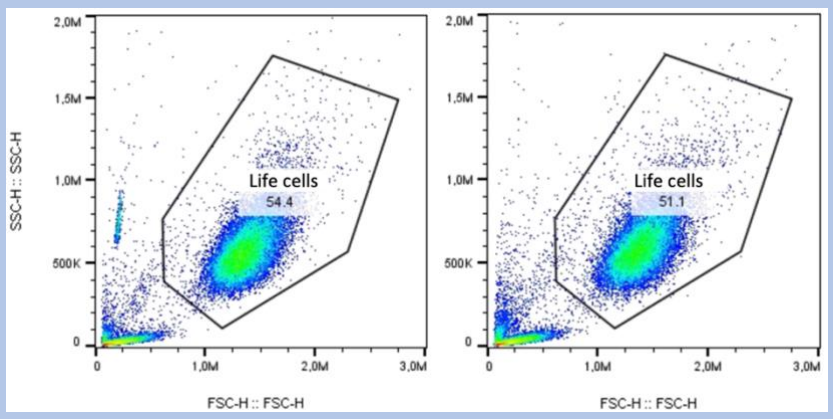

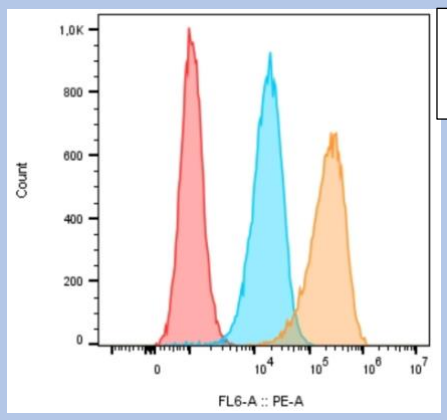

Red: control
Orange: liposomes
Blue: lip + cytD

C **D** **E**

Control *t = 3 h* *t = 5 h*

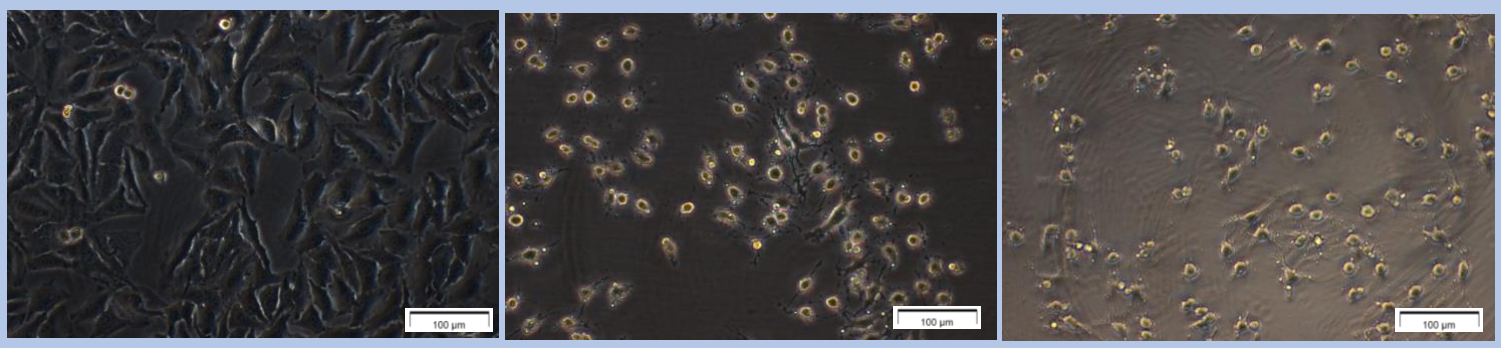

F

Figure 11: Cytochalasin D to block actin polymerization. *HeLa cells were pre-incubated for 20 minutes with 2.5 µg/mL cytochalasin D in cMEM and afterwards exposed to 50 µg/mL negatively charged liposomes with 2.5 µg/mL cytochalasin D for increasing time points. The cell fluorescence was measured using flow cytometry. The results are the average of two duplicates of each person. The blue and orange lines represent replicates of the cell fluorescent intensity of negative liposomes in HeLa cells. The yellow and grey lines represent the cell fluorescent intensity of HeLa cells exposed to chlorpromazine. The dots on each time point represent the duplicates from each person. A) Cell fluorescence intensity plot as a function of time. B) Data of (A) normalized for the uptake of liposomes in control cells without cytochalasin D. The blue and orange bars are replicates of each other. The error bars present the standard error of duplicate results. C) Scattering of cells with fluorescently labeled liposomes presented in SSC-H against FSC-H for control cells and D) for cells treated with cytochalasin D after 3 hours. E) Difference in cell fluorescence distribution with (blue) and without (orange) treatment of cytochalasin D. F) Microscopic pictures of HeLa cells exposed to 2.5 µg/mL cytochalasin D for different time points.*

Already after 1 h the cell fluorescence is reduced to around 15% (figure 11B). This decreases over time. After 3 h the cell fluorescence only 10% which remains the same after 5 h. Table 1 summarizes the mechanism of action of cytochalasin D and the different pathways that are involved in this. One of the pathways that is affected by this substance is macropinocytosis. From literature research it was suggested that macropinocytosis is mainly involved in late stages of liposome uptake into the cells (Francia et al., 2019). However, in figure 10B the inhibitory effect after 1 hour is already very strong which suggests that this inhibitor affects a pathway which is already involved in early stages of liposome uptake. From this experiment, no conclusions can be drawn because no controls have been done to see which pathway is the most affected. An explanation for the fact that the % uptake of fluorescently labeled liposomes does not reduce further than 10%, is that some dye leaked and not all the fluorescence is measured by the flow cytometer. Also, some liposomes may have stuck to the outside of the cell.

It was hypothesized that this inhibitor affects the HeLa cells since it binds actin and inhibits its polymerization (see table 1). Because actin is mainly present below the plasma membrane the cell shape will be affected. To check whether this indeed was the case, different samples were looked at under the microscope. Already after 3 h the cells looked more roundish of shape which indicates that the cell shape was altered. After 5 hours the cell almost completely lost its shape (figure 11F). The flow cytometry analysis was looked at to see whether the cells were affected in another way besides changing in shape. As can be seen in figure 11C and 11D, the SSC-H is plotted as a function of FSC-H. In figure 10C the fluorescent labeld liposomes are shown and figure 10D shows the fluorescence of liposomes with cytochalasin D after 5 hours. As can be seen in the bottom left corner there is more debris and dead cells after addition of cytochalasin D (figure 11D). However, the scattering is not affected after treatment. This suggests that cytochalasin D is not affecting the scattering of light on the cells. In figure 11E a leftward shift is observed when cytochalasin D was added together with the liposomes to the cells. This means that less fluorescently labeled liposomes are taken up by the cells when the inhibitor is added in comparison to when only liposomes are added to the cells (orange peak).

From these results it can be concluded that when cytochalasin D binds to F-actin, the cell fluorescence is inihibited for a great extent. Also, the cell shape is disrupted when this substance is added, which alters the light scatter. However, since cytochalasin D affects many pathways no real conclusions can be drawn on which pathway is mostly inhibited by this substance. Thus, it cannot be said which pathway is mostly involved in the internalization of negative liposomes into HeLa cells. A cell-based viability assay should be done to test the suggestion whether the decrease in cell fluorescence is due to toxicity. For example, a tetrazolium reduction assay can be done in which the viability of the cells is tested (Riss et al., 2013).

4.8. Uptake kinetics of liposomes with nocodazole

The next inhibitor that was analyzed was nocodazole. This inhibitor has a similar working mechanism as cytochalasin D. This substance binds to tubulin and blocks the polymerization of microtubules. Microtubules are also inside the cell and form an important interaction with actin for several processes inside the cell, among which maintenance of the cell stability (Cooper GM., 2000a; Dugina et al., 2016). Therefore, it was hypothesized that the cell shape would be disturbed after adding this inhibitor to the cells.

The cell fluorescence after addition of nocodazole was inhibited compared to the cell fluorescence of liposomes alone (figure 12A). Also, the reproducibility between me and Floris is very good and the duplicates of the both of us are almost exactly the same. It is therefore reliable to draw conclusions from these results. In figure 12D the cell fluorescence distribution is displayed. In this figure the blue peak indicates the measured fluorescently labeled liposomes. The shift of this peak to the left indicates that less fluorescence is measured after the cells were treated with nocodazole.

In figure 12B can be seen that the percentage uptake decreases over time. This can be related to the same fact as cytochalasin D, namely that one of the pathways that is involved is macropinocytosis. Despite that, the effect of this inhibitor is not as strong as that of the other inhibitors. After exposing the cells 1 h to negative liposomes with 5 µM nocodazole, the cell fluorescence is still 40%. This decreases over time to around 25 – 30% fluorescence. An explanation for this difference compared to the other inhibitors can have different reasons. Nocodazole inhibits more pathways than both chlorpromazine and cytochalasin D. Therefore, this drug may be less specific and the inhibitory effect may be not as strong as the others. It can also be that nocodazole binds covalently to tubulin. A covalent binding takes longer to make than a non-covalent binding to make. This suggest that the maximum is achieved at a time point which is not taken into account. Therefore, further measurements should be taken into account in follow-up studies.

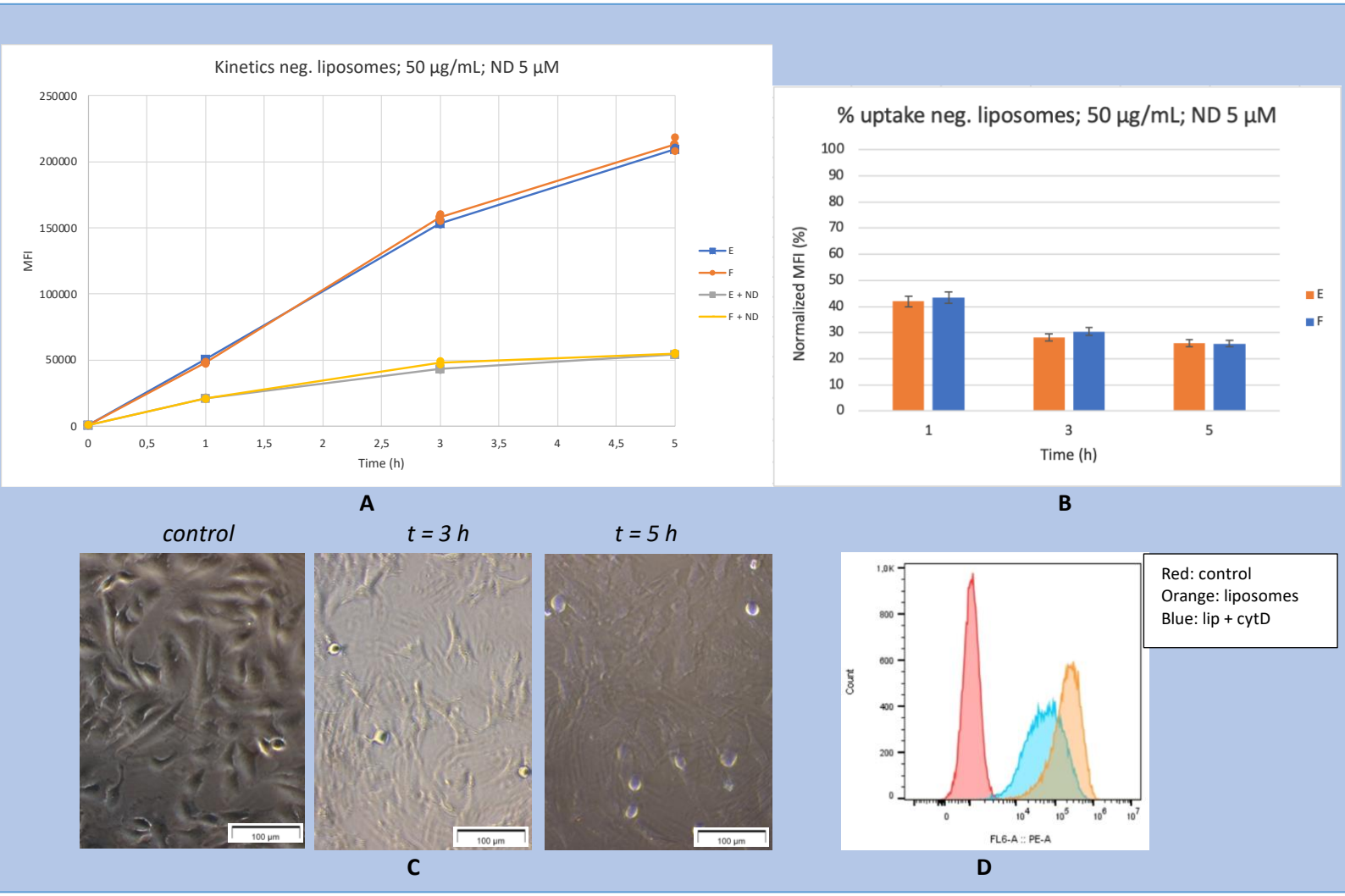

Figure 12: Nocodazole to block microtubule polymerization. *HeLa cells were pre-incubated for 20 minutes with 5 µM nocodazole in cMEM and afterwards exposed to 50 µg/mL negatively charged liposomes with 5 µM nocodazole for increasing time points. The cell fluorescence was measured using flow cytometry. The results are the average of two duplicates of each person. The blue and orange lines represent replicates of the cell fluorescent intensity of negative liposomes in HeLa cells. The yellow and grey lines represent the cell fluorescent intensity of HeLa cells exposed to nocodazole. The dots on each time point represent the duplicates from each person. A) Cell fluorescence intensity plot as a function of time. B) Data of (A) normalized for the uptake of liposomes in control cells without nocodazole. The blue and orange bars are replicates of each other. The error bars present the standard error of duplicate results. C) Microscopic pictures of HeLa cells exposed to 5 µM nocodazole for different time points. D) Difference in cell fluorescence distribution with (blue) and without (orange) treatment of nocodazole.*

The cell shape is not clearly visible on the pictures in figure 12, however it was obeserved with the eye that the cell shape did change. The cells did not looked more spherical, as was the case for cytochalasin D. However, they looked like they had shrunk. The change in cell chape can be related to the fact that microtubules interact with actin and determine the cell shape and stability.

Overall, it can be said that due to the binding of nocodazole to tubulin, the cell shape is altered. Also, less fluorescently labeled liposomes are taken up into the cells. This can be due to the contribution of multiple pathways. To check the suggestion that macropinocytosis is affecting later stages of liposome uptake into the cells, first a follow-up study needs to be done in which LDL is used as a control for CME. If liposomes are added to the cells together with LDL and these also do not show a large inhibition effect, it can be said that the inhibition of microtubule polymerization mostly affects another pathway than CME. Also, dextran can be used to check to what extent macropinocytosis contributes to the decreased cell fluorescence.

4.9. Uptake kinetics of liposomes with EIPA

To observe the effect of blocking the macropinocytosis alone, it was chosen to study EIPA next. This compound inhibits the Na+/H+ exchanger pump inside the plasma membrane, which inhibits macropinocytosis.

To test the efficacy of EIPA in inhibiting the macropinocytosis pathway, dextran was used as positive control. This substance is fluorescently labeled from itself and could be measured with the flow cytometer. As can be seen in figure 13A and 13B, the liposomes and dextran are taken up by the cells over time. After treating the liposomes with EIPA, a great inhibitory effect was observed. This was also the case when EIPA was added to dextran. Therefore, it can be concluded that dextran serves as a good control to test the efficacy of EIPA on the inhibition of macropinocytosis.

In figure 13A it can be seen that the reproducibility between me and Floris is good for every time point. No outliers are observed and which means that the duplicates almost resemble each other. Therefore, the results from this experiment are reliable to use.

The normalized MFI is displayed in figure 13C. It can be seen that for every time point the cell fluorescence is around 10%. This may suggest that EIPA already obtained its maximum effect after 45 min. In figure 12E, microscopic pictures of the cells with and without EIPA are shown. From those pictures no increase in cell death was observed. Also, under the microscope no increase in death cells was observed. No cell dead was observed, since no cell components are affected by this inhibitor that determine the cell shape or stability, also the treatment of EIPA was optimized.

Overall, it can be seen that the maximum effect of EIPA is already obtained after 45 minutes. The cell fluorescence never decreases to zero, since it can be that some dye leaked out the cytosol. Another explanation can be that the drug is stuck on the outside of the cell wall. Therefore, it can be said that when macropinocytosis is inhibited, already after 45 minutes the internalization of negative liposomes into HeLa cells is blocked.

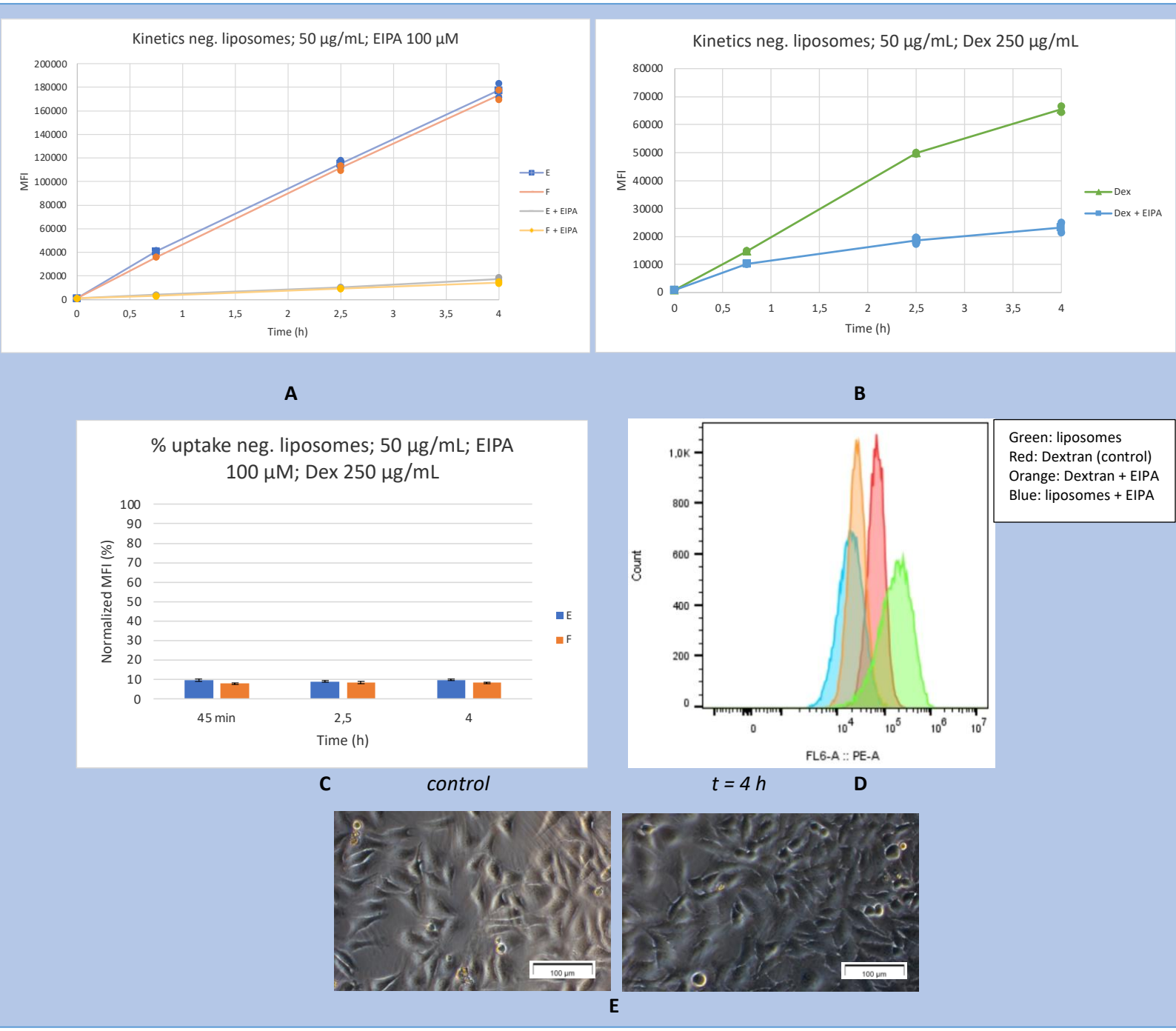

Figure 13: EIPA to inhibit macropinocytosis. *HeLa cells were pre-incubated for 20 minutes with 50 µg/mL EIPA in cMEM and afterwards exposed to 50 µg/mL negatively charged liposomes with 50 µg/mL EIPA for increasing time points. The cell fluorescence was measured using flow cytometry. The results are the average of two duplicates of each person. The blue and orange lines represent replicates of the cell fluorescent intensity of negative liposomes in HeLa cells. The yellow and grey lines represent the cell fluorescent intensity of HeLa cells exposed to nocodazole. The dots on each time point represent the duplicates from each person. A) Cell fluorescence intensity plot as a function of time. B) Cell fluorescence intensity plot as a function of time of Dextran with (blue) and without (green) EIPA. C) Data of (A) normalized for the uptake of liposomes in control cells without EIPA. The blue and orange bars are replicates of each other. The error bars present the standard error of duplicate results. D) Difference in cell fluorescence distribution of liposomes with (blue) and without (green) treatment of EIPA, and cell fluorescence distribution of dextran with (orange) and without (red) EIPA. D) Microscopic pictures of HeLa cells exposed to 50 µg/mL EIPA for different time points.*

4.10. Uptake kinetics of liposomes with MBCD and dynasore

There were two further inhibitors whose effect on the cells could be studied, dynasore and MBCD. MBCD depletes the cells cholesterol levels. Therefore, it was hypothesized that the cell loses its stability and permeability. When cell permeability is reduced, the internalization of liposomes into the cells will be inhibited. This leads to a lower cell fluorescence. Dynasore is inhibiting the protein dynamin. This protein is responsible for the fission of endocytic vesicles from the plasma membrane of cells. When the endocytic vesicle fission is inhibited, macropinocytosis is also inhibited since this is an important step in this process. Also, other pathways are affected due to this. Therefore, a lower cell fluorescence will be expected to be observed after adding this inhibitor to the cells.

A previous study found that MBCD and dynasore interact with proteins inside the serum which makes them inactive (Francia et al., 2019). That is why MBCD and dynasore followed a slightly different procedure than the other four inhibitors. The HeLa cells were pre-incubated with drugs for 1 h in serum-free medium. Subsequently, the cells were exposed to the liposomes in serum for only 30 min (see method section 3.3). It is important that the liposomes are in serum since this mimic the human body environment and you want to know how the liposomes act inside the human body. When liposomes are placed in serum-free, no protein corona will be formed around the liposomes. The protein corona however affects the distribution of the liposomes inside the human body for a huge part (Kennedy et al., 2019). Since MBCD and dynasore become inactive in serum, the exposure of liposomes with drug to HeLa cells is only done for a short period of time.

In figure 13B the fluorescent median intensity after adding dynasore and MBCD with liposomes to the cells is plotted. It can be seen that after exposing the cells to dynasore for 30 min, the cell fluorescence deceases with 80% (figure 14). For the first experiment with MBCD, the cell fluorescence was not inhibited to a great extent. We hypothesized that when the cell loses its stability and permeability due to MBCD, a greater inhibitory effect will be observed. It may be that the exposing the HeLa cells to MBCD for 30 min in serum has a negative effect on its inhibition. Therefore, this experiment was conducted for a second time to check whether this is true. This time, LacCer was used as a positive control to test the efficacy of MBCD in the depletion of cholesterol levels. LacCer is a glycosphingolipid that is found mostly in lipid rafts. Its uptake mostly is influenced by cholesterol (Zhai et al., 2006). The exact the same procedure and conditions were used as in the first experiment.

After exposing the cells to LacCer, with and without MBCD, the efficacy of the drug was observed. The results of this study are shown in figure 14A and 14B. Also, for these experiments the reproducibility between me and Floris is good. The standard deviation is also not very high. Therefore, these results are reliable to use.

It can be seen that the cell fluorescence was inhibited to a great extent in the second experiment. The suggestion that the activity of MBCD was lost after 30 minutes of incubation in medium with serum can therefore be rejected. The stock concentrations in both experiments were re-calculated and determined to be 50 mg/mL. After dilution of the stock concentration, 2.5 mg/mL MBCD was supposed to be used. An explanation for the difference in uptake between those two experiments can be that a pipetting mistake was made in the first experiment when diluting the stock concentration (figure 14B). It may be possible that instead of 2.5 mg/mL, 0.25 mg/mL MBCD was added to the liposomes. If this is really what happened, this explains the high MFI in the first experiment. By depleting the cholesterol levels, the uptake of LacCer into the cells decreased to around 50% (figure 14A). Therefore, it can be concluded that LacCer is suitable to use to determine whether cholesterol depletion by the inhibitor was effective or not.

In figure 14C, the cell fluorescent distribution of MBCD and dynasore are presented together. As can be seen for both MBCD as dynasore, the cell count is around 9000. There was a mistake made with the settings on the flow cytometer and the analysis was stopped when 20.000 cells were measured in total. However, the flow cytometer needs to measure 20.000 cells within the gate. Therefore, only 9000 cells remained after analyzing the results. From 9000 cells still a reliable result can be obtained.

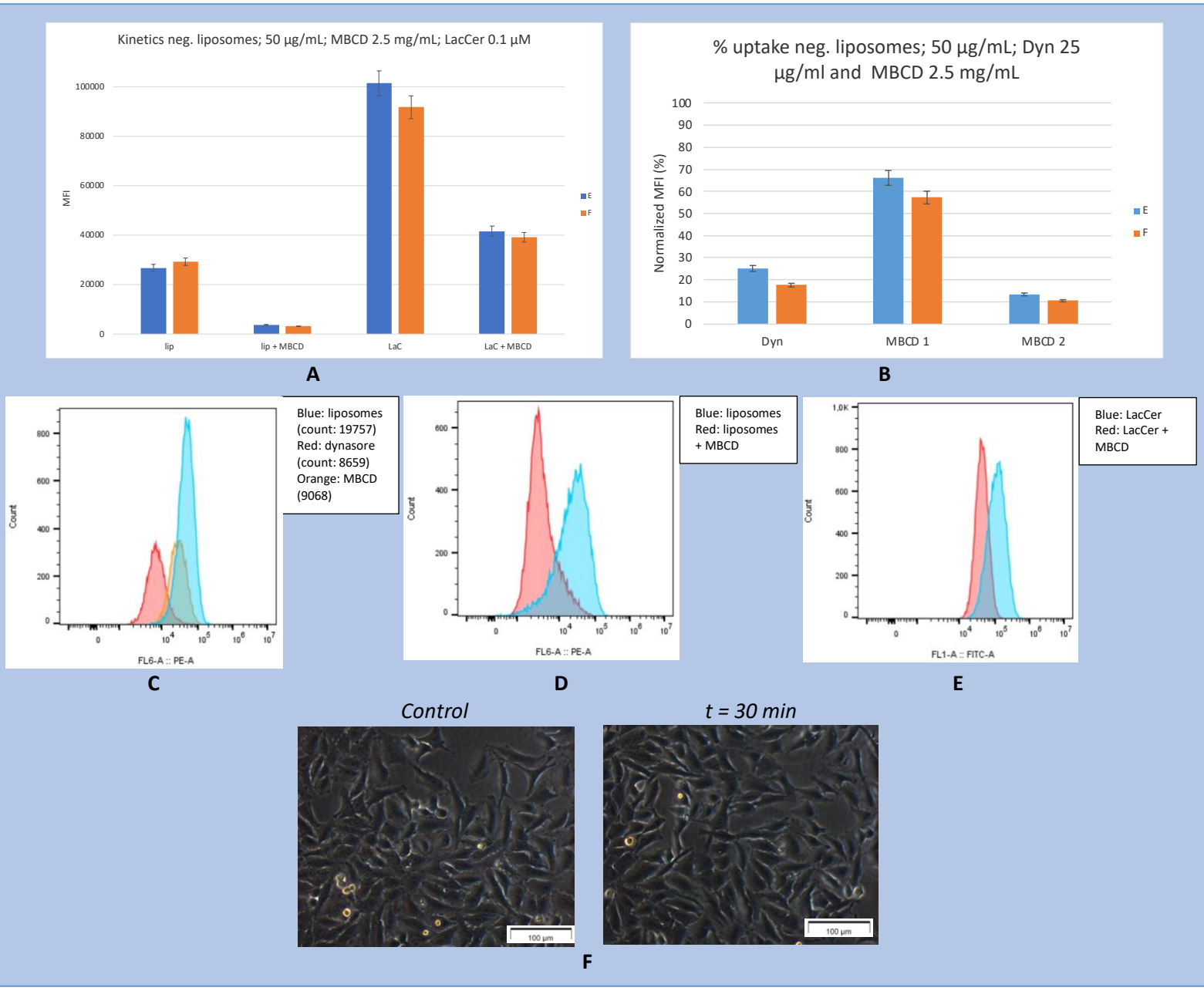

Figure 14: Dynasore to inhibit dynamin and MBCD to deplete cholesterol levels. *HeLa cells were pre-incubated for 1 h with 25 µg/mL dynasore and 2.5 mg/mL MBCD in SF-MEM and afterwards exposed to 50 µg/mL negatively charged liposomes with 25 µg/mL dynasore and 2.5 mg/mL MBCD in cMEM for increasing time points. The cell fluorescence was measured using flow cytometry. The results are the average of two duplicates of each person. The blue and orange bars are replicates of each other. The error bars present the standard error of duplicate results. A) Cell fluorescence intensity bar chart for liposomes and LacCer with and without MBCD. LacCer was used as positive control in a concentration of 0.1 µM. B) Data of (A) normalized for the uptake of liposomes in control cells without dynasore and MBCD. Difference in cell fluorescence distribution of liposomes with C) dynasore (red), with MBCD (orange) and without (blue) treatment. D) with MBCD (red) and without (blue). E) Difference in cell fluorescence distribution of LacCer with MBCD (red) and without MBCD (blue). F) Microscopic pictures of HeLa cells exposed to 2.5 mg/mL MBCD in cMEM.*

Figure 14D represents the cell fluorescent distribution of liposomes with and without MBCD. Figure 14E shows the distribution of LacCer with and without MBCD. In figure 14C, 14D and 14E a leftward shift is observed after addition of the drugs. This means that the cell fluorescence is reduced after treating the cells with dynasore and MBCD.

When comparing the microscopic pictures of HeLa cells with and without MBCD to each other, no difference in cell shape is observed. This suggests that the cell shape is not affected due to cholesterol depletion for these concentrations of MBCD.

Overall, it can be concluded that cholesterol depletion does lower the cell fluorescence. This may be due decreased cell permeability. However, multiple pathways are affected. Also, the inhibition of dynamin reduces internalization of liposomes. This indicates that inhibition of the fission of endocytic vesicles affects many entry pathways.

5. Conclusion

The aim of this research was to get a better understanding of the factors that play a role in the entry pathway of negative liposomes into cells in vivo. First, it was confirmed that the liposomes were taken up by the HeLa cells. After pre-incubating the cells for 20 minutes with NaAz, the cell fluorescence decreased of around 50%, while after pre-incubation for 1.5 h with NaAz, the cell fluorescence decreased to 20%. This effect was maintained over time. However, more debris and dead cells were observed when SSC-H was plotted against FSC-H. This suggest the decreased cell fluorescence may be due to dead cells. It can therefore not be determined what percentage between 50 and 20% of transport goes through active transport. A previous study found that pre-incubation for 30 min with NaAz reduced the internalization of negative liposomes into cells with 90%, however these liposomes had a different composition (Montizaan et al., 2020). Therefore, it is expected that pre-incubation for 20 min is too short and 1.5 h is too long. To check whether this is true for these liposomes, a follow-up study must be done in which the cells are pre-incubated for a shorter time than 1.5 hours, but longer than 20 minutes. However, since the cell fluorescence decreased in both experiments with 50% or more, it can be said that a great part of uptake depends on active processes. How much of this reduction is due to the inhibition of cellular ATP cannot be said, since also other factors can influence this decrease. These factors include that most of the cells died after 1.5 h of pre-incubation and therefore no liposomes could be internalized into the cell anymore. Another explanation is that a small percentage of the decrease in cell fluorescence is related to the fact that some liposomes had stuck on the outside of the cell or that some dye leaked out of the cytosol.

The six inhibitors that were used, were already optimized in a previous study and all of them were determined to be effective (Francia et al., 2019). Inhibition of specifically CME, by chlorpromazine, reduced the cell fluorescence to 10% after 1 h. However, over time a slight increase of 20 – 30% in cell fluorescence was observed after 5 h. A possible interpretation may be that this increase over time is due to the cationic amphiphilic behaviour of the molecule. It could also be that clathrin mediated endocytosis is only acting on early stages of liposome internalization into cells. Lastly, it may be that other pathways are upregulated over time. However, it can be concluded from this that a huge part of the internalization of negative liposomes into HeLa cells depends on the active pathway CME.

Other drugs that also affect CME, act via inhibition of actin (cytochalasin D) and microtubule (nocodazole) polymerization, however these drugs also affect other pathways. Exposure to both drugs reduced the cell fluorescence. By binding to the ends of F-actin, the actin polymerization was inhibited to such an extent that the maximum effect of cytochalasin D was already obtained after 1 hour. For nocodazole, a decrease in cell fluorescence was observed. However, this decrease was negligibly small, around 15%. When actin polymerization was blocked, the internalization of liposomes into cells seemed to be decreased even more than after blockage of microtubule polymerization. The blockage of actin polymerization resembled the decrease in cell fluorescence compared to blockage of specifically CME. This may suggest that CME is the main pathway affected when actin polymerization is blocked. A factor that may play a role is that microtubules are more dynamic than actin. It may be that the cell permeability is maintained for a longer time due to this (Cooper GM., 2000a; Dugina et al., 2016). Therefore, it takes longer to inhibited the internalization of liposomes into HeLa cells. Another factor can be that the blockage of microtubule polymerization may have more effect on other pathways, such as macropinocytosis which are also affected by nocodazole. From literature it was suggested that this pathway was upregulated in later stages of liposome uptake (Francia et al., 2019). In follow-up studies dextran should be used as a positive control for macropinocytosis. It is also useful to add transferrin and low-density lipoproteins (LDL) to check to what extent CME is inhibited. From these results it can be concluded that the internalization of liposomes into HeLa cells does depend on actin and microtubules. By inhibiting the polymerization of them, CME is affected for a huge part. Another pathway that also may be affected is macropinocytosis.

The inhibition of the Na+/H+ exchanger pump is only affecting one pathway, namely macropinocytosis. After exposing the cells to liposomes with EIPA, it looked like the maximum effect was obtained already after 45 minutes. This inhibitory effect maintained over time. This decrease in cell fluorescence is not due to toxicity inside the cells, since the treatment was already optimized and the cells did not show lysis. It can be concluded that by inhibiting the Na+/H+ exchanger pump in the plasma membrane, macropinocytosis is inhibited. This blocks the internalization of negative liposomes into the HeLa cells.

When comparing the results of cytochalasin D and EIPA, for both substances the cell fluorescence decreased to a great extent and it looked like they had already reached their maximum effect. A possible explanation for this is that macropinocytosis is responsible for most of the internalization of negative liposomes into the cells which is consistent with CME.

A previous study found that proteins inside the serum interact with MBCD and dynasore which makes them inactive. Therefore, these drugs were pre-incubated in SF-MEM and afterwards, HeLa were exposed to the drugs in serum. The efficacy of both drugs, after exposure in serum for 30 min, was also proved using LacCer and LDL as positive control (Francia et al., 2019). From the results it can be seen that the depletion of cholesterol levels inside the cell, decreases the uptake of negative liposomes to a higher extent than the uptake of LacCer. MBCD is affecting multiple pathways due to the depletion of cholesterol inside the cell. However, in the first experiment inhibition via this pathway seemed to be not very strong. After performing this experiment for the second time, the cell fluorescence decreased to around 10%. Both MBCD experiments were performed on two different days. Because all the parameters were exactly the same, it is hard to say what caused this difference. It may be that the liposomes had a slightly different concentration which caused corona proteins to faster attach to the outside of the liposome, which made the drug inactive in serum even faster. Despite the fact that both experiments had a different outcome, the reproducibility and the duplicates were good in the second experiment. It can be concluded that by depleting the cells cholesterol levels, internalization of the negative liposomes into the cells was inhibited.

By inhibiting dynamin, with dynasore, many pathways of internalization are affected. After 30 minutes, an inhibitory effect of around 80% in cell fluorescence was observed, which is consistent with the previous obtained results. It can therefore be concluded, that the internalization of negative liposomes into cells does depend on the involvement of dynamin and thus on the fission of endocytic vesicles from the plasma membrane. To obtain the maximum effect of dynasore, it may be that the drug needs to be exposed to the cells in serum for an even shorter period of time. However, further studies need to be done to prove this.

Overall, it can be concluded that several factors contribute to the internalization of liposomes into HeLa cells. EIPA showed that macropinocytosis is one of the main pathways involved in the internalization of negative liposomes into HeLa cells. By inhibiting the polymerization of actin, the result was consistent with that of EIPA. This suggests that macropinocytosis is the main internalization pathway after binding to F-actin. When AP2 was inhibited, by chlorpromazine, the internalization of liposomes was inhibited to a great extent. However, over time it seemed that the effect of inhibition fades away. This suggests that CME is only acting on the early stages of liposome uptake. Nocodazole was not consistent with any of the results. This inhibitor showed a slight decrease in cell fluorescence over time, suggesting that CME is not the main pathway affected by this inhibitor. It may be that because microtubules are more dynamic than actin, the inhibition takes longer. Through the suppression of dynamin by dynasore, and the inhibition of the microtubule network by nocodazole, vesicular trans-monolayer transfer was demonstrated.

To better understand the different factors that play a role in internalization, different controls such as LDL, transferrin and dextran should be used in experiments with inhibitors which affect multiple pathways. In follow-up research also different parameters need to be altered to determine the effect of for example particle size and surface charge of the liposome. When a liposome is positively charged, polyelectrolytes and cell membrane phospholipids will interact with each other which affects the internalization pathway. Also, some studies showed that the uptake kinetics of nanoparticles increased when the surface area was bigger. An explanation for this is that the larger surface area forms multivalent interactions with the cells (Bannunah et al., 2014; Gratton et al., 2008). When the surface area is changed, the uptake kinetics will also be affected. The pathways that are involved in the internalization of bigger particles will also be different. Consequently, it is important to investigate this. Since some inhibitors lost their efficacy over time in serum, it is useful to use different analytical methods to prove via which pathways they act. For example, mass spectrometry is a useful method which is used for analyzing liposomes in serum. This explains how lipids bind to membrane proteins and aids in the unraveling of binding mechanisms. Also, methods such as fluorescence imaging or RNA interference can be used. In follow-up research it is also important that cell viability assays are performed to check whether the decrease in cell fluorescence really depends on the inhibition of specific factors, or that the cells showed lysis (Francia et al., 2019; Frick & Schmidt, 2019).

6. References

1. Akbarzadeh, A., Rezaei-Sadabady, R., Davaran, S., Joo, S. W., Zarghami, N., Hanifehpour, Y., Samiei, M., Kouhi, M., & Nejati-Koshki, K. (2013). Liposome: classification, preparation, and applications. *Nanoscale Research Letters*, *8*(1), 102. https://doi.org/10.1186/1556-276X-8-102
2. Allen, T. M., & Cullis, P. R. (2013). Liposomal drug delivery systems: From concept to clinical applications. *Advanced Drug Delivery Reviews*, *65*(1), 36–48. https://doi.org/10.1016/j.addr.2012.09.037
3. Avanti Polar Lipids (2022). 1,2-Dioleoyl-*sn*-glycero-3-phospho-*rac*-(1-glycerol) sodium salt. Retrieved June 17, 2022 from https://avantilipids.com/product/840475
4. Avanti Polar Lipids (2022). Cholesterol (ovine wool, >98%). Retrieved June 17, 2022 from https://avantilipids.com/product/700000
5. Bannunah, A. M., Vllasaliu, D., Lord, J., & Stolnik, S. (2014). Mechanisms of Nanoparticle Internalization and Transport Across an Intestinal Epithelial Cell Model: Effect of Size and Surface Charge. *Molecular Pharmaceutics*, *11*(12), 4363–4373. https://doi.org/10.1021/mp500439c
6. Beltrán-Gracia, E., López-Camacho, A., Higuera-Ciapara, I., Velázquez-Fernández, J. B., & Vallejo-Cardona, A. A. (2019). Nanomedicine review: clinical developments in liposomal applications. *Cancer Nanotechnology*, *10*(1), 11. https://doi.org/10.1186/s12645-019-0055-y
7. Binarová, P., & Tuszynski, J. (2019). Tubulin: Structure, Functions and Roles in Disease. *Cells*, *8*(10), 1294. https://doi.org/10.3390/cells8101294
8. Blajeski, A. L., Phan, V. A., Kottke, T. J., & Kaufmann, S. H. (2002). G1 and G2 cell-cycle arrest following microtubule depolymerization in human breast cancer cells. *Journal of Clinical Investigation*, *110*(1), 91–99. https://doi.org/10.1172/JCI13275
9. Canton, J. (2018). Macropinocytosis: New Insights Into Its Underappreciated Role in Innate Immune Cell Surveillance. *Frontiers in Immunology*, *9*. https://doi.org/10.3389/fimmu.2018.02286
10. Caracciolo, G. (2015). Liposome–protein corona in a physiological environment: Challenges and opportunities for targeted delivery of nanomedicines. *Nanomedicine: Nanotechnology, Biology and Medicine*, *11*(3), 543–557. https://doi.org/10.1016/j.nano.2014.11.003
11. Cheng, C., Trzcinski, O., & Doering, L. C. (2014). Fluorescent labeling of dendritic spines in cell cultures with the carbocyanine dye â€œDiIâ€ *Frontiers in Neuroanatomy*, *8*. https://doi.org/10.3389/fnana.2014.00030
12. Cooper GM. (2000a). Microtubules. In *The Cell: A Molecular Approach. 2nd edition.* (2nd edition).
13. Cooper GM. (2000b). Structure and Organization of Actin Filaments. In *The Cell: A Molecular Approach. 2nd edition.* (2nd edition).
14. Dugina, V., Alieva, I., Khromova, N., Kireev, I., Gunning, P. W., & Kopnin, P. (2016). Interaction of microtubules with the actin cytoskeleton via cross-talk of EB1-containing +TIPs and γ-actin in epithelial cells. *Oncotarget*, *7*(45), 72699–72715. https://doi.org/10.18632/oncotarget.12236
15. Francia, V., Reker-Smit, C., Boel, G., & Salvati, A. (2019). Limits and challenges in using transport inhibitors to characterize how nano-sized drug carriers enter cells. *Nanomedicine*, *14*(12), 1533–1549. https://doi.org/10.2217/nnm-2018-0446
16. Frick, M., & Schmidt, C. (2019). Mass spectrometry—A versatile tool for characterising the lipid environment of membrane protein assemblies. *Chemistry and Physics of Lipids*, *221*, 145–157. https://doi.org/10.1016/j.chemphyslip.2019.04.001

17. Godlee, C., & Kaksonen, M. (2013). From uncertain beginnings: Initiation mechanisms of clathrin-mediated endocytosis. *Journal of Cell Biology*, *203*(5), 717–725. https://doi.org/10.1083/jcb.201307100
18. Gratton, S. E. A., Ropp, P. A., Pohlhaus, P. D., Luft, J. C., Madden, V. J., Napier, M. E., & DeSimone, J. M. (2008). The effect of particle design on cellular internalization pathways. *Proceedings of the National Academy of Sciences*, *105*(33), 11613–11618. https://doi.org/10.1073/pnas.0801763105
19. Ishikawa, T., Zhu, B.-L., & Maeda, H. (2006). Effect of sodium azide on the metabolic activity of cultured fetal cells. *Toxicology and Industrial Health*, *22*(8), 337–341. https://doi.org/10.1177/0748233706071737
20. Kennedy, D. C., Gies, V., Jezierski, A., & Yang, L. (2019). Effects of human serum on the stability and cytotoxicity of silver nanoparticles. *SN Applied Sciences*, *1*(11), 1510. https://doi.org/10.1007/s42452-019-1480-6
21. Lin, X. P., Mintern, J. D., & Gleeson, P. A. (2020). Macropinocytosis in Different Cell Types: Similarities and Differences. *Membranes*, *10*(8), 177. https://doi.org/10.3390/membranes10080177
22. Montizaan, D., Yang, K., Reker-Smit, C., & Salvati, A. (2020). Comparison of the uptake mechanisms of zwitterionic and negatively charged liposomes by HeLa cells. *Nanomedicine: Nanotechnology, Biology and Medicine*, *30*, 102300. https://doi.org/10.1016/j.nano.2020.102300
23. Onishchenko, N., Tretiakova, D., & Vodovozova, E. (2021). Spotlight on the protein corona of liposomes. *Acta Biomaterialia*, *134*, 57–78. https://doi.org/10.1016/j.actbio.2021.07.074
24. Riss, T., Moravec, R., & Niles, A. (2013). *Assay Guidance Manual [Internet]: Vol. Updated July 1, 2016* (S. Markossian, A. Grossman, & K. Brimacombe, Eds.). Eli Lilly & Company and the National Center for Advancing Translational Sciences.
25. Royle, S. J. (2006). The cellular functions of clathrin. *Cellular and Molecular Life Sciences*, *63*(16), 1823–1832. https://doi.org/10.1007/s00018-005-5587-0
26. Schliwa, M. (1982). Action of cytochalasin D on cytoskeletal networks. *Journal of Cell Biology*, *92*(1), 79–91. https://doi.org/10.1083/jcb.92.1.79
27. Sharma, A. (1997). Liposomes in drug delivery: Progress and limitations. *International Journal of Pharmaceutics*, *154*(2), 123–140. https://doi.org/10.1016/S0378-5173(97)00135-X
28. SigmaAldrich (2022). 18:1 (Δ9-Cis) PC (DOPC). Retrieved June 17, 2022 from https://www.sigmaaldrich.com/NL/en/product/avanti/850375p
29. Singh, M., Jadhav, H. R., & Bhatt, T. (2017). Dynamin Functions and Ligands: Classical Mechanisms Behind. *Molecular Pharmacology*, *91*(2), 123–134. https://doi.org/10.1124/mol.116.105064
30. Stetefeld, J., McKenna, S. A., & Patel, T. R. (2016). Dynamic light scattering: a practical guide and applications in biomedical sciences. *Biophysical Reviews*, *8*(4), 409–427. https://doi.org/10.1007/s12551-016-0218-6
31. Zhai, X., Li, X.-M., Momsen, M. M., Brockman, H. L., & Brown, R. E. (2006). Lactosylceramide: Lateral Interactions with Cholesterol. *Biophysical Journal*, *91*(7), 2490–2500. https://doi.org/10.1529/biophysj.106.084921